Preprints.org

Article

Not peer-reviewed version

Thermostable D-Allulose 3-Epimerase for Long-Term Food-Compatible Continuous Production Systems

Jiawei Cui , Yan Li * , Ming Yan *

Posted Date: 3 June 2025

doi: 10.20944/preprints202506.0243.v1

Keywords: D-allulose; D-allulose 3-epimerase; Thermogemmatispora carboxidivorans; immobilization; continuous production

Preprints.org is a free multidisciplinary platform providing preprint service that is dedicated to making early versions of research outputs permanently available and citable. Preprints posted at Preprints.org appear in Web of Science, Crossref, Google Scholar, Scilit, Europe PMC.

Copyright: This open access article is published under a Creative Commons CC BY 4.0 license, which permit the free download, distribution, and reuse, provided that the author and preprint are cited in any reuse.

Preprints.org (www.preprints.org) | NOT PEER-REVIEWED | Posted: 3 June 2025 doi:10.20944/preprints202506.0243.v1

Disclaimer/Publisher's Note: The statements, opinions, and data contained in all publications are solely those of the individual author(s) and contributor(s) and not of MDPI and/or the editor(s). MDPI and/or the editor(s) disclaim responsibility for any injury to people or property resulting from any ideas, methods, instructions, or products referred to in the content.

Article

Thermostable D-Allulose 3-Epimerase for Long-Term Food-Compatible Continuous Production Systems

Jiawei Cui, Yan Li * and Ming Yan *

Nanjing Tech University, Nanjing 211816, China

* Correspondence: liyan@njtech.edu.cn (Y.L.); yanming@njtech.edu.cn (M.Y.)

Abstract: D-allulose is a rare sugar with promising applications in food and health industries, owing to its low caloric value and multiple health benefits. In this study, we systematically investigated a thermostable D-allulose 3-epimerase (TcDAEase) from *Thermogemmatispora carboxidivorans* for food-compatible continuous production. The enzyme exhibited remarkable thermostability, with over 70% activity retained at 80 °C, and showed broad pH tolerance across the range of 8.0 to 13.0. Notably, TcDAEase exhibited high catalytic activity toward D-allulose and D-fructose even without addition of metal ions. Moreover, Food-grade Mg^{2+} was identified as enhancing enzyme activity by 14.3%, thus ensuring compliance with GRAS (Generally Recognized as Safe) standards for food applications. To improve industrial applicability, the enzyme was immobilized using a chitosan-diatomaceous earth (DE) matrix via a three-step adsorption–crosslinking–embedding strategy. The immobilized TcDAEase achieved 48.7% ± 2.4% activity recovery and retained 90.3% ± 1.5% activity over seven reaction cycles. Furthermore, continuous production of D-allulose was realized in a packed-bed reactor, operating stably at 60 °C, pH 8.0 and 5 mM Mg^{2+} for 150 days, producing 756 kg of D-allulose with a conversion yield exceeding 89.7% of the theoretical maximum. Overall, this study provides a feasible strategy for the continuous and efficient production of high value-added D-allulose in the food industry.

Keywords: D-allulose; D-allulose 3-epimerase; *Thermogemmatispora carboxidivorans*; immobilization; continuous production

1. Introduction

In recent decades, the global prevalence of metabolic disorders such as obesity, diabetes, and cardiovascular diseases has surged, primarily due to high-fat and high-sugar dietary patterns[1,2]. In response, consumer preferences have shifted toward healthier sweetening alternatives, including erythritol, acesulfame and stevia, which offer low- or zero-calorie profiles [3,4]. Among them, D-allulose (also known as D-psicose), a rare monosaccharide and the C-3 epimer of D-fructose, has garnered increasing attention owing to its favorable nutritional and physiological properties. D-allulose retains approximately 70% of the sweetness of sucrose while providing only 0.4 kcal/g of energy. In addition to its low caloric contribution, D-allulose has been shown to offer a range of health benefits, such as anti-obesity effects [5], modulation of cholesterol metabolism [6] and support for gut microbiota homeostasis [7]. These attributes position D-allulose as a highly promising functional sweetener for food and nutraceutical applications [8].

Despite its advantages, D-allulose is scarce in nature and its chemical synthesis typically requires harsh conditions and generates undesirable byproducts, limiting scalability [9,10]. As a result, biocatalytic methods offer a cleaner, more sustainable, and cost-effective route [11]. Among these, enzymatic conversion using ketose 3-epimerases, particularly D-tagatose 3-epimerase (DTEase, EC 5.1.3.31) and D-allulose 3-epimerase (DAEase, EC 5.1.3.30)has become the most viable industrial-scale production method for D-allulose [12].

To date, more than 20 microbial DAEases have been identified from various genera such as *Arthrobacter globiformis* M30 [13], *Clostridium bolteae* [14], *Ruminococcus sp.*[15] and *Bacillus subtilis* [16]

© 2025 by the author(s). Distributed under a Creative Commons CC BY license.

Preprints.org (www.preprints.org) | NOT PEER-REVIEWED | Posted: 3 June 2025 doi:10.20944/preprints202506.0243.v1

with their catalytic properties summarized in Table 1. However, most of these enzymes display limited thermostability, with optimal activity typically below 50 °C. This low-temperature requirement constrains their application in high-temperature processes, which are desirable in industry for improving substrate solubility, reducing viscosity and suppressing microbial contamination [17]. Furthermore, many reported DAEases require divalent metal cofactors such as Co^{2+} or Mn^{2+} for activation. These ions, despite their catalytic roles, are either toxic or disallowed in food processing, thereby limiting the practical use of such enzymes in food-related manufacturing processes [18]. Consequently, there remains a pressing need for the discovery and engineering of novel DAEases that combine high thermostability with activation by food-grade metal ions such as Mg^{2+} or Ca^{2+}.

In recent years, various immobilization strategies have been explored to improve the performance of DAEases [19], yet challenges remain. Li et al. [20] developed a DNA-origami-based co-immobilization platform integrating DAEase and glucose isomerase, enabling one-pot cascade conversion of glucose to D-allulose with minimal byproduct formation (reduced by approximately 80%). Tang et al. [21] reported a ZnCo-MOF-based immobilized DAEase with enhanced thermostability (80% activity retention at 70 °C) and reusability (over 95% after 8 cycles), attributed to Zn^{2+}/Co^{2+} coordination-induced structural stabilization. However, the high cost and complexity of such nanomaterials limit their industrial applicability. Alternatively, several studies have explored traditional immobilization platforms, such as chitopearl beads and ion-exchange resins [13,22], enabling medium-term continuous operation for 60-120 days. Nevertheless, few systems have demonstrated stable catalytic performance beyond 100 days under food-compatible conditions, underscoring the need for robust and durable immobilized biocatalysts.

In this study, we characterized and immobilized a novel thermostable D-allulose 3-epimerase (TcDAEase) from *Thermogemmatispora carboxidivorans*. The enzyme exhibited high catalytic efficiency, remarkable thermostability, and activation by GRAS-approved Mg^{2+}, thereby satisfying key requirements for industrial application. A cost-effective immobilization strategy based on chitosan and diatomaceous earth was further developed, enabling long-term continuous production of D-allulose in a packed-bed reactor over 150 days. This work provides a scalable and sustainable solution to the enzyme and process level limitations in the production of D-allulose.

Table 1. Comparison of biochemical properties of reported DAEases and DTEases.

Strain of enzyme source	Optimal temperature (°C)	Optimal pH	Metal ion	Half-life	Catalytic activity (U/mg)	Reference
Pseudomonas sp.	60	7.0-9.0	NR	NR	NR	[23]
Pseudomonas cichorii	60	7.5	NR	NR	NR	[24]
Agrobacterium tumefaciens	50	8.0	Mn^{2+}	63.5 min/50 °C	8.89	[25]
Sinorhizobium sp.	40	8.5	Mn^{2++}	11050 min/35 °C, 934 min/40 °C, 251 min/45 °C, 1151 min/50 °C	NR	[26]
Rhodobacter sphaeroides	40	9.0	Mn^{2+}	NR	NR	[27]
Clostridium cellulolyticum	55	8.0	Co^{2+}	408 min/60 °C	NR	[28]
Ruminococcus sp.	60	7.5-8.0	Mn^{2+}	96 min/60 °C	8.95	[15]
Clostridium sp.	65	8.0	Co^{2+}	15 min/60 °C	NR	[29]
Clostridium scindens	60	7.5	Mn^{2+}	108 min/50 °C	NR	[30]
Desmospora sp.	60	7.5	Co^{2+}	NR	NR	[31]
Clostridium bolteae	55	7.0	Co^{2+}	156 min/55 °C	NR	[14]
Dorea sp.	70	6.0	Co^{2+}	NR	803	[32]
Treponema primitia	70	8.0	Co^{2+}	30 min/60 °C	NR	[33]

© 2025 by the author(s). Distributed under a Creative Commons CC BY license.

Preprints.org (www.preprints.org) | NOT PEER-REVIEWED | Posted: 3 June 2025 doi:10.20944/preprints202506.0243.v1

Flavonifractor plautii	65	7.0	Co^{2+}	40 min/65 °C	20	[34]
Arthrobacter globiformis	70	7.0-8.0	Mg^{2+}	NR	23.6	[13]
Agrobacterium sp.	55-60	7.5-8.0	Co^{2+}	267 min/55 °C, 28.2 min/60 °C, , 3.8 min/65 °C	90.5	[35]
Corynebacterium glutamicum	55	8.0	Mn^{2+}	140 min/60 °C	22.7	[36]
DaeM	80	7.0	Co^{2+}	9900 min/60 °C, 3240 min/70 °C, 49 min/80 °C	1.14 ± 0.048	[16]
Caballeronia fortuita	65	7.5	Co^{2+}	427.8 min/50 °C, 307.8 min/55 °C, 63 min/60 °C	270 ± 1.5	[37]
Arthrobacter psychrolactophilus	70	8.5	Mg^{2+}	128.4 min/70 °C	14.3	[38]
Blautia produca	55	8.0	Mn^{2+}	180 min/55 °C	1.76 ± 0.099	[39]
Thermogemmatispora carboxidivorans	80	10.0	Ni^{2+}	720 min/60 °C, 300 min/70 °C, 40 min/80 °C	7.9 ± 0.3	This work

* NR, not reported.

2. Materials and Methods

2.1. Materials and Strains

TcDAEase gene (NCBI accession: WP_052889376.1) was synthesized by General Biologicals Corporation (Anhui, China). Escherichia coli BL21 (DE3) was utilized as the host strain for recombinant expression and was obtained from Vazyme Biotech Co., Ltd. (Nanjing, China). Substrates including D-allulose, D-tagatose, D-sorbose, and D-fructose were sourced from Sigma-Aldrich (St. Louis, MO, USA). The diatomaceous earth carrier was supplied by Yuantong Mineral Products Co. (Jilin, China), and chitosan was purchased from Aladdin Biochemical Technology Co. (Shanghai, China). All other analytical-grade reagents were acquired from Tokyo Chemical Industry (TCI), Acros Organics, and Macklin Biochemical Co., Ltd.

2.2. Amino Acid Sequence Alignment

Multiple sequence alignment of TcDAEase with other reported D-allulose 3-epimerases was conducted using Clustal Omega to identify conserved catalytic residues and structural stability. A phylogenetic tree was constructed using MEGA X via the maximum likelihood method with 1000 bootstrap replications to assess evolutionary relationships and statistical confidence.

2.3. Gene Cloning, Expression and Purification of TcDAEase

The gene sequence for TcDAEase (NCBI ID: WP_052889376.1) was inserted into the pET22b (+) vector to construct the pET22b-TcDAEase recombinant plasmid, which was subsequently introduced into *E. coli* BL21 (DE3) for heterologous expression. Pre-cultures were grown in 100 mL Luria–Bertani (LB) medium supplemented with 50 μg/mL ampicillin at 37 °C 200 rpm overnight. The seed culture was then inoculated (2% v/v) into 100 mL auto-induction Terrific Broth (15 g/L tryptone, 25 g/L yeast extract, 10 g/L NaCl, 2 g/L glucose, 3 g/L lactose). Cultures were incubated at 37 °C until OD_{600} reached 0.6, then shifted to 25 °C for 24 h to enhance protein yield. Cells were harvested via

© 2025 by the author(s). Distributed under a Creative Commons CC BY license.

Preprints.org (www.preprints.org) | NOT PEER-REVIEWED | Posted: 3 June 2025 doi:10.20944/preprints202506.0243.v1

centrifugation (8000 rpm, 4 °C, 20 min), lysed by ultrasonic disruption (60% amplitude, 1 s on/2 s off, 10 min on ice), and the lysate was clarified by centrifugation and 0.22 μm filtration. The supernatant was purified using a 5 mL nickel-affinity chromatography column equilibrated with 50 mM phosphate buffer (500 mM NaCl, pH 8.0). The enzyme was eluted using a linear imidazole gradient (0-500 mM), concentrated via centrifugal ultrafiltration (22 kDa MWCO), and dialyzed against 50 mM phosphate buffer (pH 8.0). SDS-PAGE with Coomassie Brilliant Blue staining was employed to confirm protein size and purity.

2.4. Enzyme Assay

Enzymatic activity was measured in 1.0 mL reactions containing 50 mM sodium phosphate buffer (pH 8.0) and 50 g/L D-fructose. Reactions were initiated by adding purified enzyme and incubated at 60 °C for 5 min. Termination was achieved by adding 100 μL of 1 M HCl and immediately freezing at -80 °C. Sugar concentrations were analyzed via HPLC equipped with a refractive index (RI) detector, using a calcium-form carbohydrate column (Benson Polymeric, USA) at 80 °C with deionized water as the mobile phase (flow rate: 0.6 mL/min). The sample injection volume was 10 μL, the total run time was 20 min. Protein concentration was determined by the Bradford assay, and one unit (U) of enzymatic activity was defined as the amount of enzyme required to generate 1 μmol of D-allulose per minute under the specified conditions. All measurements were performed in triplicate and reported as mean ± SD.

2.5. Biological Characteristics of TcDAEase

To simulate native conditions relevant to food-compatible applications, no metal chelation pretreatment was employed. Optimal temperature was determined by performing assays at 50-90 °C in 10 °C increments, while thermostability was evaluated by pre-incubating enzyme samples (without substrate) at 60, 70, and 80 °C in phosphate buffer, followed by activity measurement at intervals up to 8 hours.

The pH dependence was assessed using five buffer systems (50 mM): citrate-phosphate (pH 4.0-5.0), phosphate (pH 6.0-8.0), glycine-NaOH (pH 9.0-10.0), carbonate (pH 11.0), and KCl-NaOH (pH 12.0-13.0). Enzyme pH stability was tested by 6 h incubation at 60 °C across these buffers.

To evaluate metal ion effects, divalent cations (1 mM final concentration; Fe^{2+}, Co^{2+}, Ni^{2+}, Cu^{2+}, Zn^{2+}, Ca^{2+}, Mg^{2+}, Mn^{2+}) were added individually. Additionally, the Mg^{2+} dose-dependence was assessed at 0-25 mM concentrations to determine its catalytic enhancement profile.

2.6. Substrate Specificity and Kinetic Parameters

The substrate specificity of TcDAEase was evaluated against four ketohexose substrates: D-fructose, D-allulose, D-sorbose and D-tagatose. Each reaction was conducted under the standard assay conditions (60 °C, pH 8.0), and the specific activities for each substrate were determined. The relative activity was calculated by setting the activity toward D-fructose as 100%. For kinetic analysis, initial reaction rates were measured at varying concentrations of D-fructose ranging from 5 to 300 mM. The Michaelis–Menten kinetic parameters, including the Michaelis constant (K_m), turnover number (k_{cat}), and catalytic efficiency (k_{cat}/K_m), were determined by nonlinear regression fitting of the rate data to the Michaelis–Menten equation using OriginPro 9.0. All assays were performed in triplicate, and results were expressed as mean ± SD.

2.7. TcDAEase Immobilization Procedure

The bacteria used for enzyme immobilization were cultivated as described in Section 2.2. A three-step adsorption–crosslinking–embedding approach was employed using a chitosan–diatomaceous earth (DE) composite as the support matrix. Briefly, chitosan (10 g/L) was dissolved in 1% (v/v) acetic acid with constant stirring. Diatomaceous earth (100 g/L) and glutaraldehyde (0.5 g/L) were added, and the pH was adjusted to 4.5 using 1 M NaOH to activate the support. Wet biomass

© 2025 by the author(s). Distributed under a Creative Commons CC BY license.

Preprints.org (www.preprints.org) | NOT PEER-REVIEWED | Posted: 3 June 2025 doi:10.20944/preprints202506.0243.v1

was then added at the desired concentration, followed by gentle stirring at 25 °C for 1 h to facilitate adsorption. Chitosan precipitation was induced by gradually adjusting the pH using either 1 M NaOH or 1.4 M Na_2SO_4 to reach one of three target pH ranges: acidic (5.0-6.0), neutral (6.5-7.0) or alkaline (10.0-11.0). To enhance mechanical strength, 1.4 M Na_2SO_4 was used for osmotic dehydration, after which the immobilized material was filtered, washed thoroughly with deionized water, and dried at 60 °C for 2 h until a constant weight was achieved. The final immobilized enzyme preparation was stored at 4 °C until use. To optimize immobilization efficiency and operational stability, three key parameters were systematically investigated. The effects of wet cell loading (5-30 g/L), chitosan precipitation pH (5.0-6.0, 6.5-7.0, and 10.0-11.0), and chitosan concentration (5-40 g/L) were investigated. For each condition, protein loading capacity and activity recovery were quantified. The enzyme activity of the immobilized preparations was determined under standard assay conditions. The activity recovery (%) of the immobilized TcDAEase was calculated as the ratio between the specific activity ($U \cdot g^{-1}$) of the immobilized preparation and that of the corresponding amount of free wet cells. Breakpoint analysis and first-order kinetic fitting were applied to model saturation and decay trends for protein loading and catalytic activity, respectively.

2.8. Characterization of Immobilized TcDAEase

The biochemical performance of the immobilized enzyme was evaluated following the same methodology as used for the free enzyme. Specifically, temperature profiles were measured at 50-90 °C, while pH activity profiles were assessed at 60 °C using the buffer systems described in Section 2.5. Operational stability was evaluated through repeated batch conversions. In each cycle, immobilized TcDAEase was incubated in 50 g/L D-fructose solution (pH 8.0, containing 5 mM $MgCl_2$) at 60 °C with shaking at 100 rpm for 2 h. After each cycle, the catalyst was recovered by centrifugation, washed with phosphate buffer (pH 8.0) and reused. This procedure was repeated for seven consecutive cycles. The residual activity was calculated based on the initial activity measured in the first batch, which was set as 100%.

2.8. Production of D-Allulose by a Continuous Packed-Bed Reactor

A jacketed packed-bed column reactor (2.0 cm inner diameter × 30 cm height) was filled with 30 g of immobilized TcDAEase (particle size 0.5-1.0 mm; bulk density ~0.7 g/mL). The system was maintained at a constant temperature of 60 °C using a circulating water-ethanol bath (70:30 v/v). The substrate solution, comprising 500 g/L D-fructose and 5 mM $MgCl_2$ in 50 mM sodium phosphate buffer (pH 8.0), was pumped through the reactor at a flow rate of 30 mL/min, resulting in an empty-bed residence time (EBRT) of 1.3 min. Effluent samples were collected every 24 h, filtered through 0.22 μm membranes, and analyzed by HPLC as described in Section 2.4 to determine substrate conversion and residual enzyme activity.

3. Results and Discussion

3.1. Amino Acid Sequence Alignment of TcDAEase

TcDAEase exhibited considerable sequence divergence from previously characterized DAEases. As shown in Figure 1, TcDAEase shared amino acid sequence identities from12.0% to 48.08% with other known DAEases, with the highest similarity observed for the enzyme derived from *Arthrobacter globiformis*. Domain architecture analysis classified TcDAEase as a member of the xylose isomerase-like family (IPR036237). Multiple sequence alignment (Figure 2) revealed several conserved residues that are functionally important for the isomerization of D-fructose [40]. These include Glu149, Asp182, His208, and Glu243 [33], which participate in metal ion coordination, and residues Glu156, His185, and Arg214, which are involved in anchoring the O1, O2, and O3 positions of D-fructose [34]. These findings suggest that TcDAEase preserves the core structural features essential for efficient ketose epimerization.

© 2025 by the author(s). Distributed under a Creative Commons CC BY license.

Preprints.org (www.preprints.org) | NOT PEER-REVIEWED | Posted: 3 June 2025 doi:10.20944/preprints202506.0243.v1

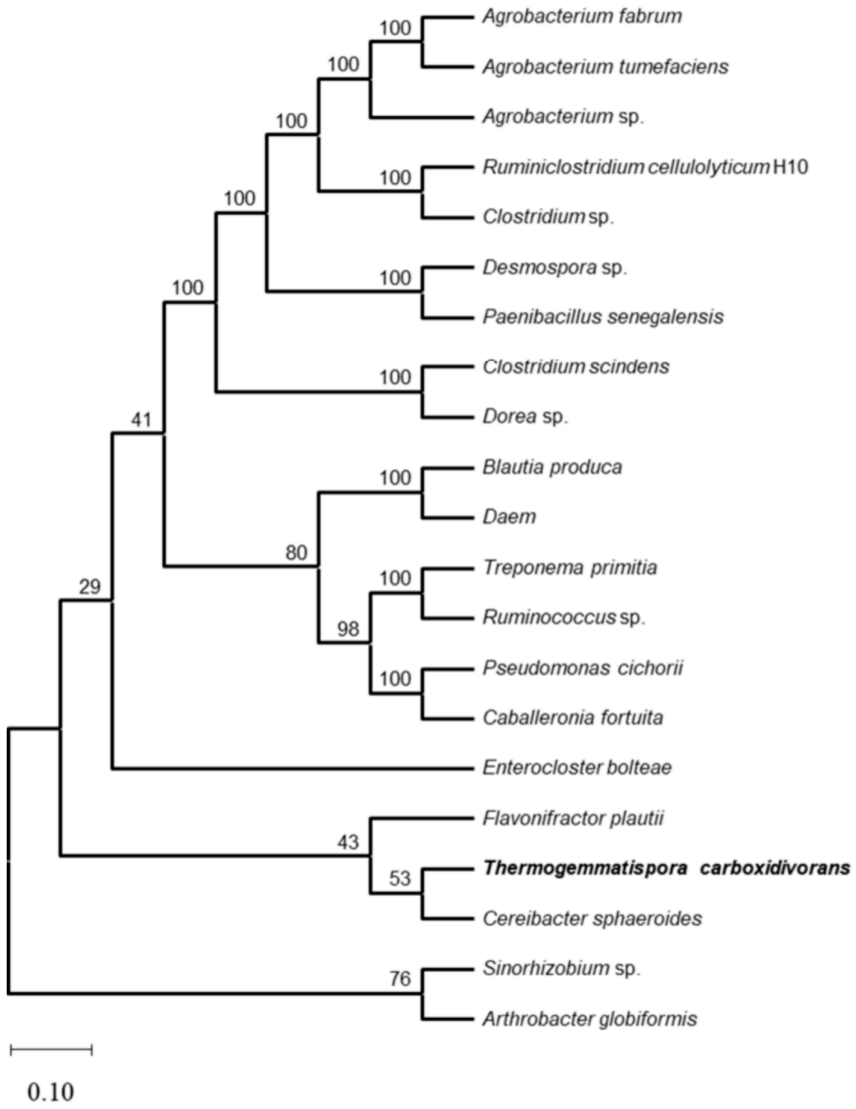

Figure 1. Phylogenetic tree showing evolutionary relationships between TcDAEase and other reported D-allulose and D-tagatose epimerases. The amino acid sequence sources were as follows: *Thermogemmatispora carboxidivorans* (WP_052889376.1); *Agrobacterium fabrum* (AAK88700.1); *Enterocloster bolteae* (EDP19602.1); *Ruminiclostridium cellulolyticum* H10 (ACL75304.1); *Treponema primitia* (ZP_09717154.1); *Desmospora* sp. (WP_009711885.1); *Clostridium* sp. (WP_014314767.1); *Clostridium scindens* (WP_004607502.1); *Ruminococcus* sp. (ZP_04858451.1); *Cereibacter sphaeroides* (ACO59490.1); *Pseudomonas cichorii* (BAA24429.1); *Agrobacterium* sp. (EGL65884.1); *Flavonifractor plautii* (WP_007494289.1); *Paenibacillus senegalensis* (WP_010270828.1); *Caballeronia fortuita* (WP_061137998.1); *Sinorhizobium* sp. (WP_069063284.1); *Agrobacterium tumefaciens* (ANH56792.1); Dorea sp.(WP_022318236.1) *DaeM* (WP_010270828.1); and *Blautia produca* (WP_294524766.1).

© 2025 by the author(s). Distributed under a Creative Commons CC BY license.

Preprints.org (www.preprints.org) | NOT PEER-REVIEWED | Posted: 3 June 2025 doi:10.20944/preprints202506.0243.v1

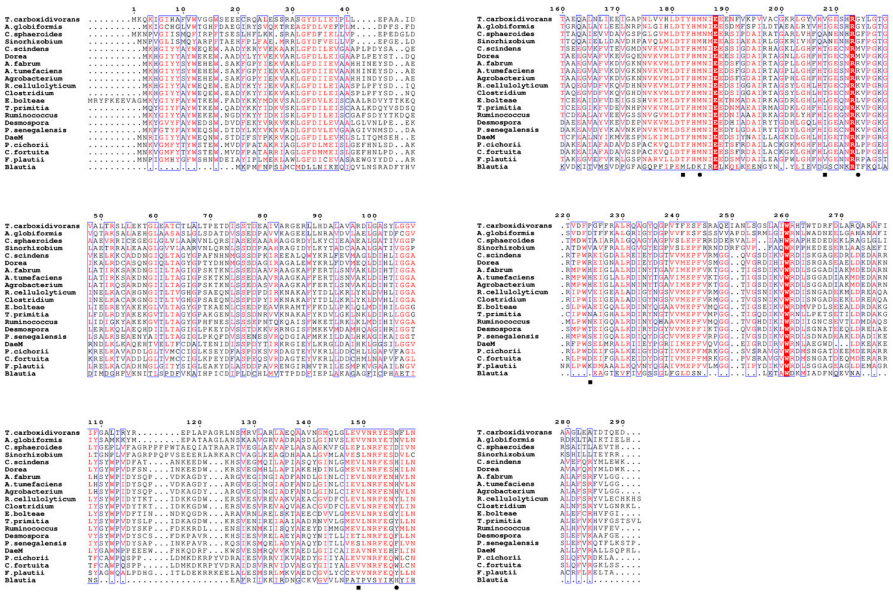

Figure 2. Multiple sequence alignment of D-allulose 3-epimerases showing conserved residues involved in metal coordination (■) and substrate binding (●). Strictly conserved amino acids are shown in red boxes. Alignment visualization was performed using ESPript 3.0.

3.2. Recombinant Expression and Biochemical Characterization of TcDAEase

The TcDAEase gene was successfully overexpressed in E. coli BL21 (DE3) and purified to homogeneity via Ni^{2+}-NTA chromatography. As shown in Figure 3 and Figure S1, the SDS-PAGE analysis revealed a distinct protein band at approximately 33 kDa, this result is consistent with the calculated molecular mass of 33.7 kDa. Notably, the purified enzyme retained high catalytic activity (7.9 ± 0.3 U·mg^{-1}) in the absence of externally supplemented metal ions, suggesting that essential cofactors may have remained bound during expression and purification. A similar phenomenon has also been observed in DAEases from *Arthrobacter globiformis* M30 [13] and *Clostridium bolteae* [14], which exhibited baseline activity under metal-free conditions, although their maximal activity was achieved upon Co^{2+} addition. This intrinsic activity highlights the enzyme's potential for food-compliant biocatalysis.

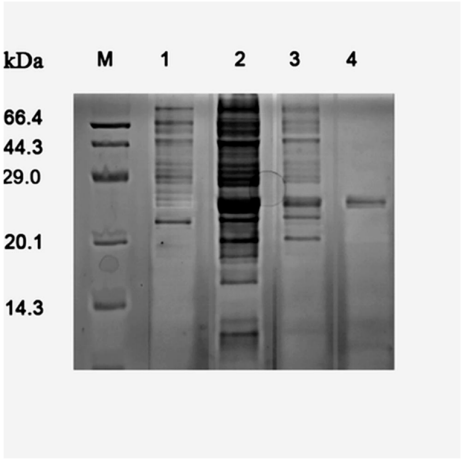

Figure 3. SDS-PAGE analysis of recombinant TcDAEase expression and purification. Lane M: Protein molecular weight marker (14.3-66.4 kDa); Lane 1: *E. coli* BL21 (DE3) (empty pET-22b vector); Lane 2: *E. coli* BL21 (DE3) expressing TcDAEase; Lane 3: crude cell extract; Lane 4: purified TcDAEase.

© 2025 by the author(s). Distributed under a Creative Commons CC BY license.

Preprints.org (www.preprints.org) | NOT PEER-REVIEWED | Posted: 3 June 2025 doi:10.20944/preprints202506.0243.v1

3.3. Thermostability, pH Tolerance and Metal Ion Dependence

The enzymatic properties of TcDAEase were evaluated under the conditions described in Section 2.4. As shown in Figure 4a, TcDAEase exhibited optimal activity at 80 °C and retained over 70% of its activity within the 60-90 °C range. Thermal inactivation analysis (Figure 4b) revealed half-lives of 720 min at 60 °C, 300 min at 70 °C, and 40 min at 80 °C, indicating superior thermostability compared to most previously reported DAEases. As summarized in Table 1, TcDAEase outperformed other DAEases in terms of thermal resistance, underscoring its potential for high-temperature industrial applications.

In terms of pH tolerance, TcDAEase displayed a broad activity profile with an optimum at pH 10.0. Notably, more than 70% of its maximal activity was retained across the pH range of 8.0–13.0, whereas activity declined sharply below pH 5.0 (Figure 4c). Long-term pH stability tests (Figure 4d) showed that the enzyme remained stable after 6 h incubation at 60 °C between pH 7.0 and 9.0. Although TcDAEase tolerated strongly alkaline conditions, maintaining the reaction environment below pH 9.0 is advisable to avoid non-enzymatic browning, particularly in food-related processes [41].

The effects of various metal ions on enzymatic activity were assessed by supplementing 1 mM of different divalent cations (Figure 4e). Among them, Ni^{2+}, Co^{2+}, and Mg^{2+} enhanced catalytic activity by 30.3%, 20.2%, and 14.3%, respectively. While Ni^{2+} exhibited the strongest activation effect, its toxicity and regulatory limitations preclude its application in food-grade systems [18]. In contrast, Mg^{2+} is FDA-GRAS approved and thus suitable for industrial use. Further investigations on Mg^{2+} concentration (Figure 4f) revealed that enzymatic activity increased with Mg^{2+} concentration and plateaued beyond 5 mM. Accordingly, 5 mM Mg^{2+} was selected as the optimal cofactor concentration for continuous D-allulose production.

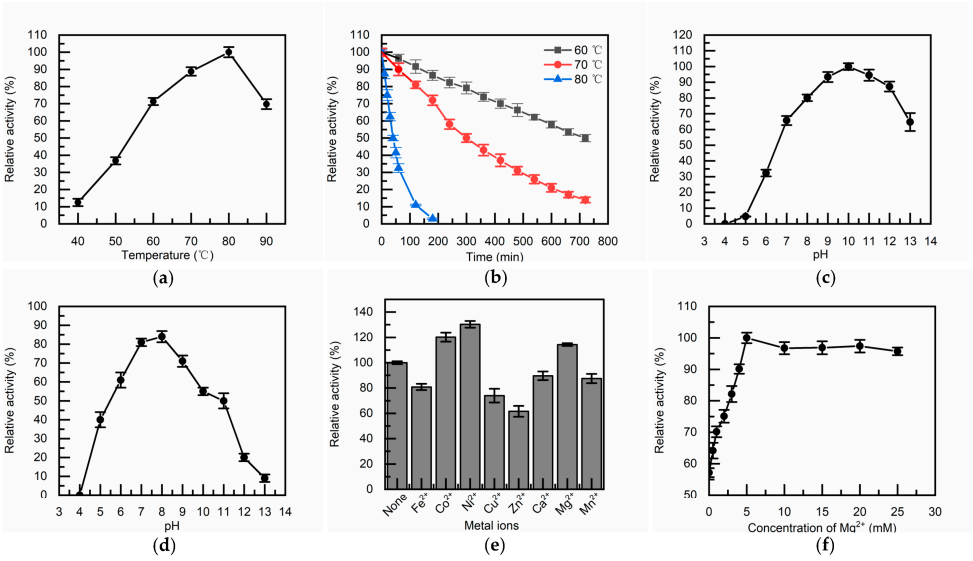

Figure 4. Effect of temperature, pH, and metal ions on TcDAEase activity. The investigation of optimal temperature (a) and thermal stability (b) employed a buffer solution of 50 mM NaH_2PO_4-Na_2HPO_4 (pH 8.0) supplemented with 1 mM Mg^{2+}; the effect of pH was conducted using various buffers: Na_2HPO_4-citrate buffer (pH 4.0-5.0), Na_2HPO_4-NaH_2PO_4 buffer (pH 6.0-8.0), glycine-NaOH buffer (pH 9.0-10.0), Na_2CO_3-$NaHCO_3$ buffer (pH 11.0), and KCl-NaOH buffer (pH 12.0-13.0), targeting optimal pH (c) and pH stability (d); the impact of various metal ions was evaluated at 60 °C and pH 8.0, examining the optimal activating ions (e) and the influence of Mg^{2+} concentration on activity (f).

© 2025 by the author(s). Distributed under a Creative Commons CC BY license.

Preprints.org (www.preprints.org) | NOT PEER-REVIEWED | Posted: 3 June 2025 doi:10.20944/preprints202506.0243.v1

3.4. Substrate Specificity and Kinetic Parameters

The substrate specificity of TcDAEase was evaluated using four ketohexoses: D-allulose, D-fructose, D-tagatose, and D-sorbose. As shown in Figure 5, TcDAEase exhibited the highest specific activity toward D-allulose (15.9 ± 0.2 U·mg^{-1}), followed by D-fructose, D-tagatose, and D-sorbose. This substrate preference supports the hypothesis of a conserved epimerization mechanism among DAEases and is consistent with previous reports on enzymes from *Arthrobacter globiformis* M30 [13], *Clostridium scindens* [30], *Ruminococcus* sp. [15], *Clostridium* sp. [29], and *Corynebacterium glutamicum* [36], all of which showed a similar catalytic bias toward D-allulose. These findings indicate a conserved substrate recognition pattern among DAEases that likely underpins a shared catalytic mechanism [42].

The kinetic parameters of TcDAEase toward D-fructose were further determined by Michaelis–Menten analysis. The enzyme exhibited a K_m of 260.9 ± 7.4 mM, a k_{cat} of 96.6 ± 0.5 s^{-1}, and a catalytic efficiency k_{cat}/K_m of 0.38 ± 0.02 s^{-1}·mM^{-1}. A comparison with previously reported DAEases (Table 2) shows that while the kinetic performance of TcDAEase is comparable to other characterized enzymes, its combination of high activity and exceptional thermostability renders it a promising biocatalyst for large-scale, continuous D-allulose production in industrial settings.

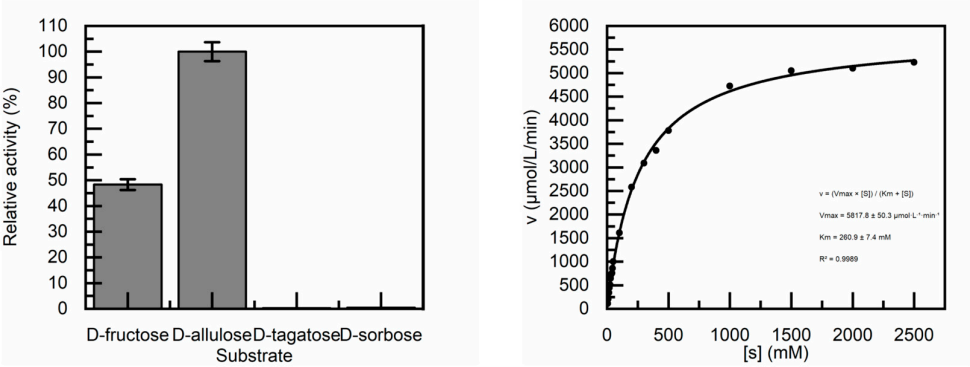

(**a**) (**b**)

Figure 5. (a) Relative activity of TcDAEase toward different D-ketohexoses, with D-allulose set as 100%; (b) Michaelis–Menten kinetic curve of TcDAEase for D-fructose.

Table 2. Comparison of the kinetic parameters of reported DAEases and DPEases.

Enzyme source (strain)	k_{cat} (s^{-1})	K_m (mM)	k_{cat}/K_m (s^{-1}·mM^{-1})	Reference
Agrobacterium tumefaciens	34.46 ± 0.46	24 ± 0.15	1.41 ± 0.02	[25]
Clostridium cellulolyticum	55.91 ± 0.787	53.5 ± 1.8	1.045 ± 0.025	[28]
Ruminococcus sp.	59.4 ± 0.483	216 ± 2	0.267 ± 0.017	[15]
Clostridium sp.	272.87 ± 1.37	279 ± 10.8	0.978 ± 0.065	[29]
Clostridium scindens	5.83 ± 0.43	40.1 ± 2.5	0.145 ± 0.02	[30]
Clostridium bolteae	59 ± 1	59.8 ± 8.2	0.99 ± 0.05	[14]
Dorea sp.	5507.45	153	3.31	[32]
Treponema primitia	292.88 ± 6.48	279 ± 20.7	1.05 ± 0.097	[33]
Flavonifractor plautii	225280	162	156	[34]
Arthrobacter globiformis	41.8	37.5	1.12	[13]
Agrobacterium sp.	106.7	110	1.06	[35]
Corynebacterium glutamicum	40.92 ± 0.175	366.7 ± 10.5	0.11 ± 0.077	[36]
Bacillus subtilis	41.99 ± 2.3	141.43 ± 7.5	0.29 ± 0.09	[16]
Caballeronia fortuita	157.21 ± 0.53	81.9 ± 4.3	1.30 ± 0.12	[37]
Arthrobacter psychrolactophilus	2920	738.7	3.953	[38]

© 2025 by the author(s). Distributed under a Creative Commons CC BY license.

Preprints.org (www.preprints.org) | NOT PEER-REVIEWED | Posted: 3 June 2025 doi:10.20944/preprints202506.0243.v1

Blautia produca	65.03 ± 3.56	235.7 ± 9.938	0.28 ± 0.014	[39]
Thermogemmatispora carboxidivorans	**96.6 ± 0.5**	**260.9 ± 7.4**	**0.38 ± 0.02**	**This work**

3.5. Immobilization Optimization and Stability Assessment of TcDAease

To achieve large-scale production of D-allulose, we optimized the immobilization process for TcDAEase and used whole-cell immobilization techniques while circumventing the cost of enzyme purification by using the natural permeability of E. coli membranes to small molecule substrates [43,44]. Drawing on immobilization studies of glucose isomerase [45,46], we developed a diatomite–chitosan composite carrier that integrates the high mechanical strength of diatomaceous earth with the strong binding capacity of chitosan. The adsorption-crosslinking-embedding process was finely controlled by adjusting pH conditions. Specifically, we used glutaraldehyde pretreatment at pH 3.0 to ensure uniform dispersion of the carrier materials, adjusted the pH to 4.5 to promote adsorption and cross-linking of the cells, and finally adjusted the pH over 5.0, a gradual alkalinisation promoted the precipitation of chitosan. Besides, the composite carrier was optimized for compatibility with packed-bed reactor applications.

We first focus on the optimization of chitosan. Chitosan is a bio-compatible binder that enhances the mechanical robustness of the matrix and prevents leaching of enzymes during manipulation. To improve the operational stability and reproducibility of the immobilized enzyme, three key parameters were systematically evaluated: wet cell loading, chitosan precipitation pH, and chitosan concentration. As shown in Figure 6a, protein loading increased linearly with cell concentration in the range of 0.5-1.52 g/100 mL (slope = 10.3 ± 0.8 mg/100 mL). Beyond this range, loading efficiency declined sharply (slope = 1.8 ± 0.3 mg/100 mL). Breakpoint analysis identified a critical saturation threshold at 1.52 ± 0.10 g/100 mL, which is consistent with the surface saturation of the carrier material [47]. In parallel, enzyme activity recovery exhibited first-order decay kinetics (k = 0.45 ± 0.05). And the half-maximal activity observed at 1.54 g/100 mL, which closely aligning with the protein loading saturation point. This strong correlation suggests that excessive cell density hinders the effective utilization of the enzyme by restricting the diffusion of crosslinking agents [48]. Additionally, spatial constraints at high cell densities may induce conformational distortions that impede substrate access and ultimately reduce catalytic efficiency [49]. According to these results, 1.5 g/100 mL was selected as the optimal cell loading, yielding a protein loading of 23 ± 0.8 mg/g and approximately 50% activity recovery. This condition offered a balanced trade-off between carrier utilization and enzyme performance. In addition, the pH for chitosan precipitation was identified as a critical factor influencing immobilization efficiency. We embedded them in three pH intervals, acidic (5.0-6.0), neutral (6.5-7.0) and basic (10.0-11.0). Although chitosan's theoretical precipitation pKa is ~6.3, partial gelation was observed even at pH 5.0-6.0, which likely due to localized pH fluctuations during NaOH titration under vigorous stirring. As shown in Figure 6b, immobilized TcDAEase prepared at pH 5.0-6.0, 6.5-7.0 and 10.0-11.0 exhibited activities of 1.4 ± 0.3, 6.7 ± 0.2 and 6.1 ± 0.2 $U \cdot g^{-1}$, corresponding to activity recoveries of 19 ± 0.5%, 49 ± 1.2% and 41 ± 1.3%, respectively. These results indicate that neutral to mildly alkaline conditions significantly enhanced catalytic performance, likely due to improved chitosan precipitation and network formation. In contrast, excessively alkaline conditions may result in over-crosslinking, which can impair enzyme conformation or hinder substrate diffusion [50]. Overall, a neutral pH range (6.5-7.0) was found to provide optimal precipitation efficiency and enzymatic activity, potentially due to the favorable protonation state of chitosan for controlled gelation and Schiff base (CH=N) formation [51].The concentration of chitosan is also one of the key factors affecting performance. Too low concentration can result in an insufficiently intact matrix, which can weaken the particle strength. Conversely, too high a concentration will result in the formation of a dense gel, which will limit matrix diffusion and thus reduce apparent activity [52]. As shown in Figure 6c,d, the highest initial activity (9.7 ± 0.9 $U \cdot g^{-1}$) was observed at a chitosan concentration of 5 g/L. However, poor operational stability was noted under this condition, with rapid activity decay (k = 0.24 ± 0.02 $cycle^{-1}$, $t_{1/2}$ = 2.9 cycles, R^2= 0.98). In contrast, increasing the chitosan

© 2025 by the author(s). Distributed under a Creative Commons CC BY license.

Preprints.org (www.preprints.org) | NOT PEER-REVIEWED | Posted: 3 June 2025 doi:10.20944/preprints202506.0243.v1

concentration to 10 g/L significantly enhanced stability ($k = 0.01 \pm 0.003$ cycle^{-1}, $t_{1/2} = 69.3$ cycles, $R^2 = 0.91$). Under these optimized conditions, 90.3 ± 1.5% of the initial activity was retained after seven consecutive cycles. This corresponds to a 24-fold reduction in the rate of inactivation compared to the 5 g/L condition. These improvements align with previous findings suggesting that a critical chitosan concentration (~8 g/L) is required to establish a percolation threshold for network formation on silica-based supports [53].

In summary, under optimized conditions (wet cell loading: 15 g/L; precipitation pH: 6.5–7.0; chitosan concentration: 10 g/L), the immobilized TcDAEase achieved 49 ± 1.2% activity recovery and demonstrated favorable mechanical integrity. As shown in Figure 7, the enzyme prepared via the three-step method exhibited excellent operational stability, with no detectable protein leaching after drying and repeated washing at 60 °C. These findings confirm the successful formation of a robust immobilization matrix, whose particles after filtration are shown in Figure S2.

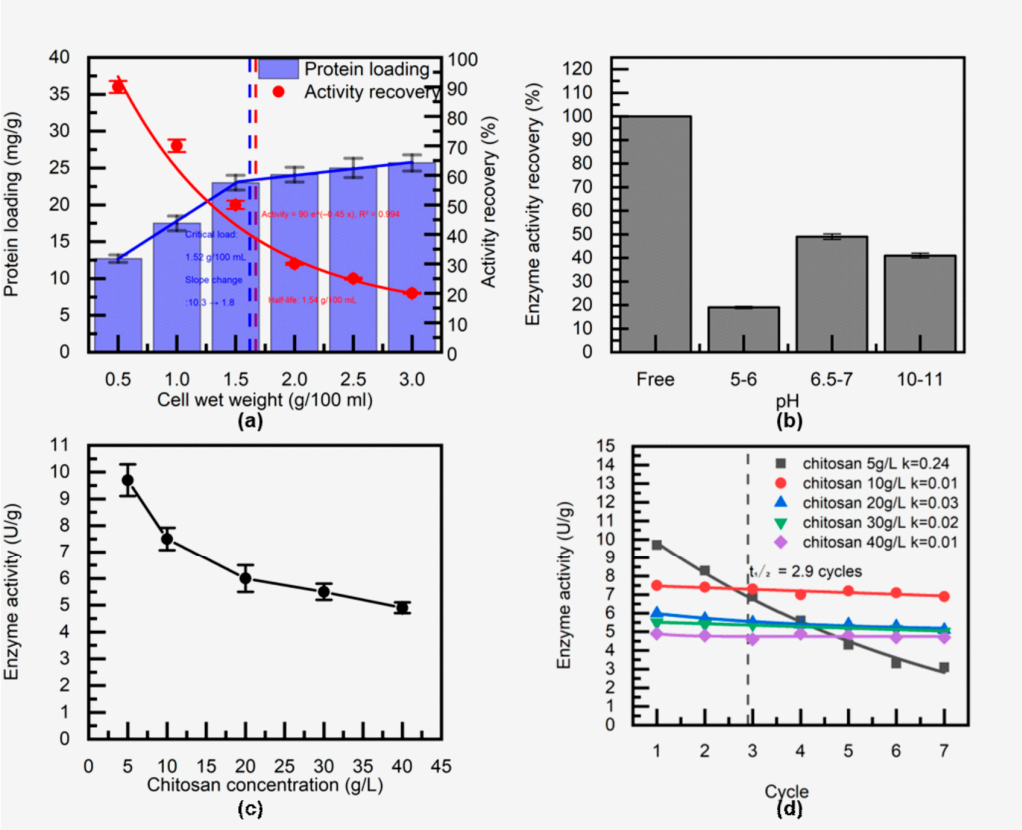

Figure 6. Optimization of TcDAEase immobilization parameters. (a) Effect of wet cell loading (0.5-2.5 g/100 mL) on protein loading and activity recovery; (b) Immobilized enzyme activity at different precipitation pH values: 5.0–6.0 (adjusted with 1 M NaOH and 1.4 M Na_2SO_4), 6.5–7.0 (adjusted by gradual addition of 1 M NaOH), and 10.0–11.0 (adjusted by excess addition of 1 M NaOH). (c) Initial catalytic activity versus chitosan concentration (2.5-10 g/L); (d) Operational stability during seven batch cycles for 5 g/L (■), 10 g/L (●), 20 g/L (▲), 30 g/L (▼), and 40 g/L (♦) chitosan concentrations.

© 2025 by the author(s). Distributed under a Creative Commons CC BY license.

Preprints.org (www.preprints.org) | NOT PEER-REVIEWED | Posted: 3 June 2025 doi:10.20944/preprints202506.0243.v1

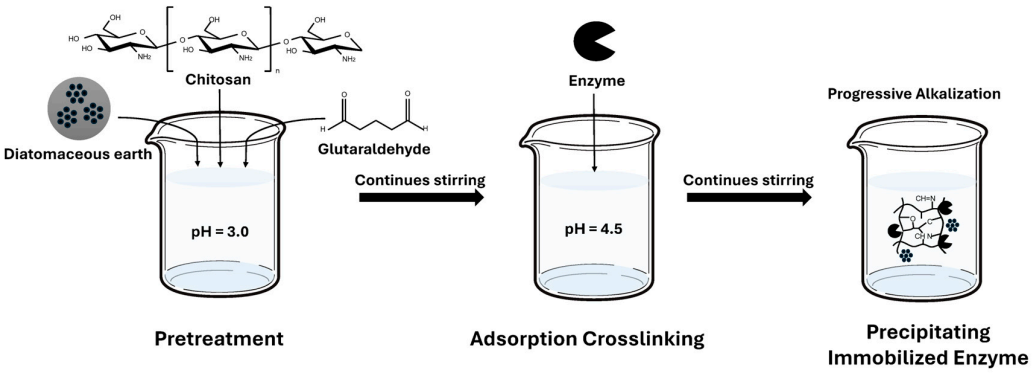

Figure 7. Schematic illustration of the three-step adsorption–crosslinking–embedding process for immobilizing TcDAEase onto a chitosan–diatomaceous earth composite.

3.6. Biochemical Properties of the Immobilized TcDAEase

The biochemical properties of immobilized TcDAEase were evaluated under optimized conditions. As shown in Figure 8a, the immobilized enzyme retained over 70% of its relative activity across the temperature range of 60–90 °C, with peak activity (over 90%) between 70 and 90 °C. Compared to the free enzyme which exhibited rapid activity loss above 80 °C, the immobilized form displayed enhanced thermal tolerance. Figure 8b illustrates that TcDAEase also retained high activity under strongly alkaline conditions, with a pH optimum above 10.0. However, from an industrial perspective, extremely high temperatures and pH values pose challenges such as increased energy consumption and the risk of non-enzymatic browning reactions (e.g., Maillard reaction), which can compromise product quality [41]. Therefore, 60 °C and pH 8.0 were selected as the optimal operating conditions, offering a balance between catalytic performance, stability, and process feasibility.

To assess operational stability, reusability tests were conducted under these conditions (60 °C, pH 8.0, 5 mM Mg^{2+}). As shown in Figure 9, immobilized TcDAEase retained 90.3% ± 1.5% of its initial activity after seven consecutive cycles—outperforming commonly used agarose- and alginate-based systems, which typically retain only 40–70% activity under similar conditions [54]. This exceptional stability is likely attributed to the synergistic effects of the composite matrix. The glutaraldehyde-crosslinked chitosan network restricts conformational mobility and protects against thermal denaturation, while the porous diatomaceous earth framework provides a large surface area and abundant binding sites, mitigating enzyme leaching and aggregation [55]. Although structural analyses such as SEM or BET were not performed, the physical properties of the composite carrier were consistent with those of food-grade diatomite materials reported in previous literature [48]. Furthermore, the hydrophilic amino and hydroxyl groups of chitosan may create a favorable microenvironment that shields the enzyme from interfacial stresses during packed-bed operation [56].

Together, these results confirm that the chitosan–diatomaceous earth matrix imparts excellent thermal and operational stability to TcDAEase, supporting its application in continuous, food-compatible, and cost-effective D-allulose biomanufacturing.

© 2025 by the author(s). Distributed under a Creative Commons CC BY license.

Preprints.org (www.preprints.org) | NOT PEER-REVIEWED | Posted: 3 June 2025 doi:10.20944/preprints202506.0243.v1

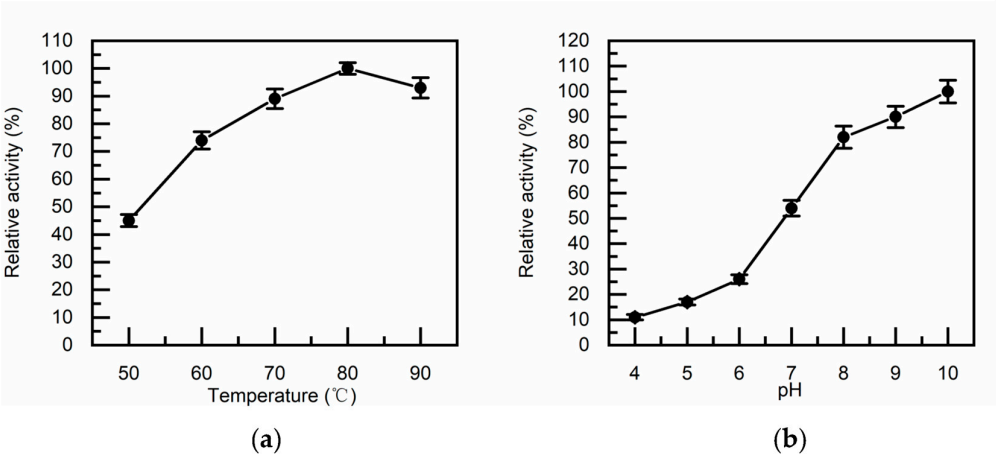

Figure 8. Biochemical characterization of immobilized TcDAEase. (a) Temperature-activity profile measured in 50 mM Na_2HPO_4-NaH_2PO_4 buffer (pH 8.0) containing 1 mM Mg^{2+}. (b) pH-activity profile assessed at 60 °C using various buffer systems (Na_2HPO_4-citrate buffer (pH 4.0-5.0), Na_2HPO_4- NaH_2PO_4 buffer (pH 6.0-8.0), glycine-NaOH buffer (pH 9.0-10.0)).

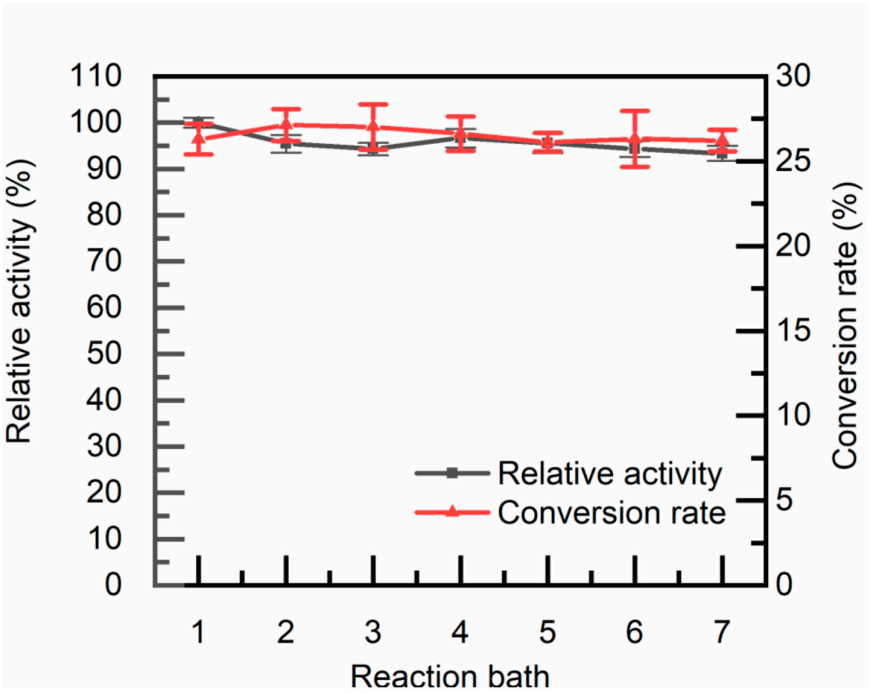

Figure 9. Reusability of immobilized TcDAEase: The reaction occurred by introducing 1 g of immobilized TcDAEase into a 20 mL fructose solution comprising 50 g/L D-fructose, 1 mM Mg^{2+}, maintained at 60 °C and pH 8.0. Following each reaction, the immobilized TcDAEase was washed with deionized water and transferred into fresh fructose solution for successive reaction batches. After each batch, residual catalytic activity (■) and substrate conversion (▲) were analyzed.

3.7. Long-Term Continuous D-Allulose Production in Packed-Bed Reactor

As a result of the above findings, 30 g of immobilized TcDAEase was loaded into a packed-bed reactor (Figure 10a) under fixed reaction conditions (60 °C, pH 8.0, 5 mM Mg^{2+}, 500 g/L D-fructose, and a flow rate of 30 mL/min) for long-term production testing. Over 150 consecutive days of

© 2025 by the author(s). Distributed under a Creative Commons CC BY license.

Preprints.org (www.preprints.org) | NOT PEER-REVIEWED | Posted: 3 June 2025 doi:10.20944/preprints202506.0243.v1

operation, the system produced a cumulative total of 756 kg of D-allulose, corresponding to 89.7% of the theoretical maximum (842.2 kg) yield.

Throughout the trial, the reactor exhibited stable hydraulic performance with no detectable pressure buildup or clogging, indicating efficient mass transfer and the mechanical robustness of the immobilized matrix. As shown in Figure 10b, the specific activity of TcDAEase gradually decreased by about 30% (from 6.5 to 4.5 U·g^{-1}), and the substrate conversion rate declined from 26.0 ± 1.2% to 22.5 ± 1.1%. These results confirm the long-term operational stability and excellent performance of the immobilized TcDAEase system for continuous, food-grade D-allulose production.

This system notably outperformed previously reported immobilized enzyme platforms. For instance, Takeshita et al. [22] achieved a 60-day operation using 200 g of immobilized D-tagatose 3-epimerase (70 U·g^{-1}), yielding only 20 kg of D-allulose at pH 7.0. Yoshihara et al. [13] reported continuous production using DAEase from *Arthrobacter globiformis* immobilized on an ion-exchange resin, which produced 215 kg of D-allulose per liter of catalyst over four months at 55 °C and pH 7.5.

Collectively, these findings underscore the scalability, durability, and industrial viability of the TcDAEase-based biocatalytic system for large-scale, continuous D-allulose manufacturing under food-compatible conditions.

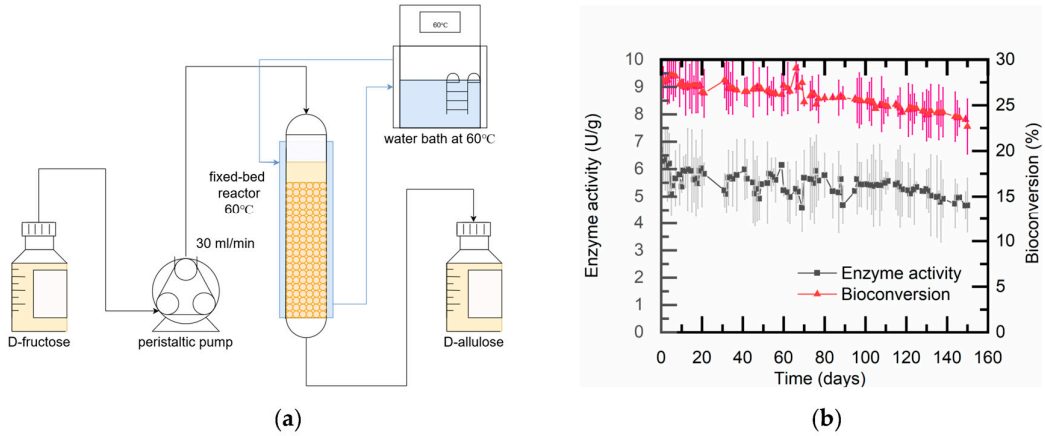

Figure 10. Continuous bioconversion of D-fructose to D-allulose by immobilized TcDAEase in a packed-bed reactor. (a) Schematic of the reactor system (30 g immobilized enzyme, 60 °C jacket temperature). (b) Operational stability over 150 days: Residual activity (▲) and conversion rate (■) were monitored under continuous conditions (30 mL/min, 500 g/L D-fructose, pH 8.0, 5 mM Mg^{2+}).

4. Conclusions

In this study, we systematically investigated the catalytic properties and industrial potential of a thermostable D-allulose 3-epimerase (TcDAEase) from Thermogemmatispora carboxidivorans. The enzyme exhibited outstanding thermostability, broad pH tolerance, and high catalytic activity toward D-allulose and D-fructose, even in the absence of metal ion supplementation. Among the tested cofactors, food-grade Mg^{2+} significantly enhanced enzymatic activity, emphasizing the suitability of TcDAEase for food-grade rare sugar production. To improve practical applicability, TcDAEase was immobilized on a chitosan–diatomaceous earth matrix, resulting in favorable activity recovery and excellent operational stability. The immobilized biocatalyst achieved an activity recovery of 48.7% ± 2.4% and retained 90.3% ± 1.5% of its initial activity after seven consecutive cycles. Remarkably, the immobilized enzyme enabled continuous D-allulose production in a packed-bed reactor for 150 days minimal decline (approximately 4%) in conversion efficiency, outperforming several previously reported systems. These results demonstrate that the integration of enzyme thermostability, food-compatible activation, and cost-effective immobilization offers a promising strategy for the scalable and sustainable production of D-allulose.

© 2025 by the author(s). Distributed under a Creative Commons CC BY license.

Preprints.org (www.preprints.org) | NOT PEER-REVIEWED | Posted: 3 June 2025 doi:10.20944/preprints202506.0243.v1

Supplementary Materials: Figure S1. Original SDS-PAGE image of TcDAEase (corresponding to Figure 3 in the main text); Figure S2. Appearance of the filtered immobilized TcDAEase particles; Figure S3. Photograph of the packed-bed re-actor system used for continuous D-allulose production.

Author Contributions: Conceptualization, M.Y. and Y.L.; methodology, J.C.; validation, J.C.; formal analysis, J.C.; investigation, J.C.; resources, M.Y. and Y.L.; data curation, J.C.; writing—original draft preparation, J.C.; writing—review and editing, J.C., M.Y. and Y.L.; visualization, J.C.; supervision, M.Y. and Y.L.; project administration, M.Y. and Y.L.; funding acquisition, M.Y. and Y.L. All authors have read and agreed to the published version of the manuscript.

Funding: This research was funded by the Guangdong Provincial Department of Science and Technology, Key-Area Research and Development Program of Guangdong Province, grant number 2022B0202120001. The APC was funded by the same grant.

Institutional Review Board Statement: Not applicable.

Informed Consent Statement: Not applicable.
Data Availability Statement: Data are contained within the article.

Acknowledgments: This study does not involve any experiments with human participants or animals and therefore did not re-quire ethical approval.

Conflicts of Interest: The authors declare no conflicts of interest.

References

1. El-Kassas, G.; Ziade, F. Exploration of the Risk Factors of Generalized and Central Obesity among Adolescents in North Lebanon. *Journal of environmental and public health* **2017**, *2017*, 2879075, doi:10.1155/2017/2879075.
2. Legler, J.; Fletcher, T.; Govarts, E.; Porta, M.; Blumberg, B.; Heindel, J.J.; Trasande, L. Obesity, Diabetes, and Associated Costs of Exposure to Endocrine-Disrupting Chemicals in the European Union. *J. Clin. Endocrinol. Metab.* **2015**, *100*, 1278-1288, doi:10.1210/jc.2014-4326.
3. Monsan, P.; Puzo, G.; Mazarguil, H. Mechanism of glutaraldehyde-protein bond formation. *Biochimie* **1975**, *57*, 1281-1292.
4. Zhang, W.; Chen, D.; Chen, J.; Xu, W.; Chen, Q.; Wu, H.; Guang, C.; Mu, W.J.C.R.i.F.S.; Nutrition. D-allulose, a versatile rare sugar: recent biotechnological advances and challenges. **2021**, *63*, 5661 - 5679.
5. Zhao, T.; Zhao, G.; Gao, F.; Zhang, Q.; Shang, S.; Lu, X.J.J.o.F.F. D-allulose attenuated metaflammation by calming adipose tissue macrophages, boosting intestinal barrier, and modulating gut microbiota in HFD mice. **2024**.
6. Yermek, R.; Wang, L.; Kaneko, K.; Han, W.; Seino, Y.; Yabe, D.; Yada, T.J.B.; communications, b.r. D-Allulose cooperates with glucagon-like peptide-1 and activates proopiomelanocortin neurons in the arcuate nucleus and central injection inhibits feeding in mice. **2022**, *613*, 159-165.
7. Hayashi, N.; Iida, T.; Yamada, T.; Okuma, K.; Takehara, I.; Yamamoto, T.; Yamada, K.; Tokuda, M. Study on the Postprandial Blood Glucose Suppression Effect of D-Psicose in Borderline Diabetes and the Safety of Long-Term Ingestion by Normal Human Subjects. *Biosci. Biotechnol. Biochem.* **2010**, *74*, 510-519, doi:10.1271/bbb.90707.
8. Teysseire, F.; Bordier, V.; Budzinska, A.; Van Oudenhove, L.; Weltens, N.; Beglinger, C.; Woelnerhanssen, B.K.; Meyer-Gerspach, A.C. Metabolic Effects and Safety Aspects of Acute D-allulose and Erythritol Administration in Healthy Subjects. *Nutrients* **2023**, *15*, 13, doi:10.3390/nu15020458.
9. Li, L.; Zhang, Q.; Wang, T.; Qi, H.; Wei, M.; Lu, F.; Guan, L.; Mao, S.; Qin, H.J.J.o.a.; chemistry, f. Engineering of Acid-Resistant d-Allulose 3-Epimerase for Functional Juice Production. **2022**, *70 51*, 16298-16306.
10. Jia, D.; Sun, C.; Peng, C.; Liu, Z.; Li, M.; Wang, H.; Chen, K.; Cheng, X.; Chen, D. Advances on D - psicose and its synthesis. *Food and Fermentation Industries* **2021**, *47*, 211-217.
11. Li, C.; Li, L.; Feng, Z.; Guan, L.; Lu, F.; Qin, H.J.F.c. Two-step biosynthesis of d-allulose via a multienzyme cascade for the bioconversion of fruit juices. **2021**, *357*, 129746.

© 2025 by the author(s). Distributed under a Creative Commons CC BY license.

Preprints.org (www.preprints.org) | NOT PEER-REVIEWED | Posted: 3 June 2025 doi:10.20944/preprints202506.0243.v1

12. Hu, M.; Li, M.; Jiang, B.; Zhang, T.J.C.r.i.f.s.; safety, f. Bioproduction of D-allulose: Properties, applications, purification, and future perspectives. **2021**.
13. Yoshihara, A.; Kozakai, T.; Shintani, T.; Matsutani, R.; Ohtani, K.; Iida, T.; Akimitsu, K.; Izumori, K.; Gullapai, P.K. Purification and characterization of D-allulose 3-epimerase derived from *Arthrobacter globiformis* M30, a GRAS microorganism. *J. Biosci. Bioeng.* **2017**, *123*, 170-176, doi:10.1016/j.jbiosc.2016.09.004.
14. Jia, M.; Mu, W.M.; Chu, F.F.; Zhang, X.M.; Jiang, B.; Zhou, L.L.; Zhang, T. A D-psicose 3-epimerase with neutral pH optimum from *Clostridium bolteae* for D-psicose production: cloning, expression, purification, and characterization. *Appl. Microbiol. Biotechnol.* **2014**, *98*, 717-725, doi:10.1007/s00253-013-4924-8.
15. Zhu, Y.M.; Men, Y.; Bai, W.; Li, X.B.; Zhang, L.L.; Sun, Y.X.; Ma, Y.H. Overexpression of D-psicose 3-epimerase from *Ruminococcus* sp. in *Escherichia coli* and its potential application in D-psicose production. *Biotechnol. Lett.* **2012**, *34*, 1901-1906, doi:10.1007/s10529-012-0986-4.
16. Patel, S.N.; Kaushal, G.; Singh, S.P. A Novel D-Allulose 3-Epimerase Gene from the Metagenome of a Thermal Aquatic Habitat and D-Allulose Production by *Bacillus subtilis* Whole-Cell Catalysis. *Appl. Environ. Microbiol.* **2020**, *86*, 14, doi:10.1128/aem.02605-19.
17. Che Hussian, C.H.A.; Leong, W.Y.J.J.o.G.E.; Biotechnology. Thermostable enzyme research advances: a bibliometric analysis. **2023**, *21*.
18. Devlin, J.J.; Pomerleau, A.C.; Brent, J.; Morgan, B.W.; Deitchman, S.D.; Schwartz, M.D.J.J.o.M.T. Clinical Features, Testing, and Management of Patients with Suspected Prosthetic Hip-Associated Cobalt Toxicity: a Systematic Review of Cases. **2013**, *9*, 405-415.
19. Xia, Y.; Cheng, Q.; Mu, W.; Hu, X.; Sun, Z.; Qiu, Y.; Liu, X.; Wang, Z.J.F. Research Advances of d-allulose: An Overview of Physiological Functions, Enzymatic Biotransformation Technologies, and Production Processes. **2021**, *10*.
20. Han, R.; Tu, W.; Liu, S.; Ji, Y.; Schwaneberg, U.; Guo, Y.; Ni, Y.J.F.B. Novel multienzyme cascade for efficient synthesis of d-allulose from inexpensive sucrose. **2023**.
21. Tang, H.; Chen, Y.; Fan, D.; Zhao, F.; Han, S.J.I.j.o.b.m. Designable immobilization of D-allulose 3-epimerase on bimetallic organic frameworks based on metal ion compatibility for enhanced D-allulose production. **2024**, 133027.
22. Takeshita, K.; Suga, A.; Takada, G.; Izumori, K. Mass production of D-psicose from D-fructose by a continuous bioreactor system using immobilized D-tagatose 3-epimerase. *J. Biosci. Bioeng.* **2000**, *90*, 453-455, doi:10.1263/jbb.90.453.
23. Izumori, K.; Khan, A.R.; Okaya, H.; Tsumura, T. A NEW ENZYME, D-KETOHEXOSE 3-EPIMERASE, FROM PSEUDOMONAS SP ST-24. *Biosci. Biotechnol. Biochem.* **1993**, *57*, 1037-1039, doi:10.1271/bbb.57.1037.
24. Ishida, Y.; Kamiya, T.; Itoh, H.; Kimura, Y.; Izumori, K. Cloning and characterization of the D-tagatose 3-epimerase gene from Pseudomonas cichorii ST-24. *J. Ferment. Bioeng.* **1997**, *83*, 529-534, doi:10.1016/s0922-338x(97)81132-4.
25. Kim, H.J.; Hyun, E.K.; Kim, Y.S.; Lee, Y.J.; Oh, D.K. Characterization of an *Agrobacterium tumefaciens* D-psicose 3-epimerase that converts D-fructose to D-psicose. *Appl. Environ. Microbiol.* **2006**, *72*, 981-985, doi:10.1128/aem.72.2.981-985.2006.
26. Oh, D.K.; Kim, N.H.; Kim, H.J.; Park, C.S.; Kim, S.W.; Ko, M.; Park, B.W.; Jung, M.H.; Yoon, K.H. D-Psicose production from D-fructose using an isolated strain, *Sinorhizobium* sp. *World J. Microbiol. Biotechnol.* **2007**, *23*, 559-563, doi:10.1007/s11274-006-9265-7.
27. Zhang, L.T.; Mu, W.M.; Jiang, B.; Zhang, T. Characterization of d-tagatose-3-epimerase from *Rhodobacter sphaeroides* that converts d-fructose into d-psicose. *Biotechnol. Lett.* **2009**, *31*, 857-862, doi:10.1007/s10529-009-9942-3.
28. Mu, W.M.; Chu, F.F.; Xing, Q.C.; Yu, S.H.; Zhou, L.; Jiang, B. Cloning, Expression, and Characterization of a D-Psicose 3-Epimerase from *Clostridium cellulolyticum* H10 (vol 59, pg 7785, 2011). *J. Agric. Food Chem.* **2013**, *61*, 10408-10408, doi:10.1021/jf404585g.
29. Mu, W.M.; Zhang, W.L.; Fang, D.; Zhou, L.; Jiang, B.; Zhang, T. Characterization of a D-psicose-producing enzyme, D-psicose 3-epimerase, from *Clostridium* sp. *Biotechnol. Lett.* **2013**, *35*, 1481-1486, doi:10.1007/s10529-013-1230-6.

© 2025 by the author(s). Distributed under a Creative Commons CC BY license.

Preprints.org (www.preprints.org) | NOT PEER-REVIEWED | Posted: 3 June 2025 doi:10.20944/preprints202506.0243.v1

30. Zhang, W.L.; Fang, D.; Xing, Q.C.; Zhou, L.; Jiang, B.; Mu, W.M. Characterization of a Novel Metal-Dependent D-Psicose 3-Epimerase from *Clostridium scindens* 35704. *PLoS One* **2013**, *8*, 9, doi:10.1371/journal.pone.0062987.
31. Zhang, W.L.; Fang, D.; Zhang, T.; Zhou, L.; Jiang, B.; Mu, W.M. Characterization of a Metal-Dependent D-Psicose 3-Epimerase from a Novel Strain, Desmospora sp 8437. *J. Agric. Food Chem.* **2013**, *61*, 11468-11476, doi:10.1021/jf4035817.
32. Zhang, W.L.; Li, H.; Zhang, T.; Jiang, B.; Zhou, L.; Mu, W.M. Characterization of a D-psicose 3-epimerase from *Dorea* sp CAG317 with an acidic pH optimum and a high specific activity. *J. Mol. Catal. B-Enzym.* **2015**, *120*, 68-74, doi:10.1016/j.molcatb.2015.05.018.
33. Zhang, W.L.; Zhang, T.; Jiang, B.; Mu, W.M. Biochemical characterization of a D-psicose 3-epimerase from *Treponema primitia* ZAS-1 and its application on enzymatic production of D-psicose. *J. Sci. Food Agric.* **2016**, *96*, 49-56, doi:10.1002/jsfa.7187.
34. Park, C.S.; Kim, T.; Hong, S.H.; Shin, K.C.; Kim, K.R.; Oh, D.K. D-Allulose Production from D-Fructose by Permeabilized Recombinant Cells of *Corynebacterium glutamicum* Cells Expressing D-Allulose 3-Epimerase *Flavonifractor plautii*. *PLoS One* **2016**, *11*, 22, doi:10.1371/journal.pone.0160044.
35. Tseng, W.C.; Chen, C.N.; Hsu, C.T.; Lee, H.C.; Fang, H.Y.; Wang, M.J.; Wu, Y.H.; Fang, T.Y. Characterization of a recombinant D-allulose 3-epimerase from *Agrobacterium* sp ATCC 31749 and identification of an important interfacial residue. *Int. J. Biol. Macromol.* **2018**, *112*, 767-774, doi:10.1016/j.ijbiomac.2018.02.036.
36. Yang, J.G.; Tian, C.Y.; Zhang, T.; Ren, C.X.; Zhu, Y.M.; Zeng, Y.; Men, Y.; Sun, Y.X.; Ma, Y.H. Development of food-grade expression system for d-allulose 3-epimerase preparation with tandem isoenzyme genes in *Corynebacterium glutamicum* and its application in conversion of cane molasses to D-allulose. *Biotechnol. Bioeng.* **2019**, *116*, 745-756, doi:10.1002/bit.26909.
37. Li, S.N.; Chen, Z.W.; Zhang, W.L.; Guang, C.E.; Mu, W.M. Characterization of a D-tagatose 3-epimerase from *Caballeronia fortuita* and its application in rare sugar production. *Int. J. Biol. Macromol.* **2019**, *138*, 536-545, doi:10.1016/j.ijbiomac.2019.07.112.
38. Laksmi, F.A.; Nirwantono, R.; Nuryana, I.; Agustriana, E. Expression and characterization of thermostable D-allulose 3-epimerase from *Arthrobacter psychrolactophilus* (Ap DAEase) with potential catalytic activity for bioconversion of D-allulose from D-fructose. *Int. J. Biol. Macromol.* **2022**, *214*, 426-438, doi:10.1016/j.ijbiomac.2022.06.117.
39. Tang, X.R.; An, Y.F.; Iqbal, M.W.; Cong, H.R.; Zhang, G.Y.; Zhang, Y.F.; Ravikumar, Y.; Zabed, H.M.; Zhao, M.; Zhou, H.X.; et al. The Characterization of a Novel D-allulose 3-Epimerase from *Blautia produca* and Its Application in D-allulose Production. *Foods* **2022**, *11*, 18, doi:10.3390/foods11203225.
40. Jumper, J.M.; Evans, R.; Pritzel, A.; Green, T.; Figurnov, M.; Ronneberger, O.; Tunyasuvunakool, K.; Bates, R.; Žídek, A.; Potapenko, A.; et al. Highly accurate protein structure prediction with AlphaFold. **2021**, *596*, 583 - 589.
41. Kathuria, D.; Hamid; Gautam, S.; Thakur, A.J.F.C. Maillard reaction in different food products: Effect on product quality, human health and mitigation strategies. **2023**.
42. Ivanova, N.S.; Kulminskaya, A.A.; Shvetsova, S.V.J.R.J.o.B.C. Structural and Functional Features of Ketose-3-Epimerases and Their Use for D-Allulose Production. **2023**, *49*, 731 - 741.
43. Guo, Q.; Zheng, L.-J.; Luo, X.; Gao, X.; Liu, C.-Y.; Deng, L.; Fan, L.-H.; Zheng, H.J.J.o.a.; chemistry, f. Engineering Escherichia coli for d-Allulose Production from d-Fructose by Fermentation. **2021**.
44. Guo, Q.; Dong, Z.-X.; Luo, X.; Zheng, L.-J.; Fan, L.-H.; Zheng, H.J.J.o.b. Engineering Escherichia coli for D-allulose biosynthesis from glycerol. **2024**.
45. Gao, X.; Wei, C.; Qi, H.; Li, C.; Lu, F.; Qin, H.J.F.c. Directional immobilization of D-allulose 3-epimerase using SpyTag/SpyCatcher strategy as a robust biocatalyst for synthesizing D-allulose. **2022**, *401*, 134199.
46. Neifar, S.; Cervantes, F.V.; Bouanane-Darenfed, A.; BenHlima, H.; Ballesteros, A.O.; Plou, F.J.; Bejar, S.J.F.c. Immobilization of the glucose isomerase from Caldicoprobacter algeriensis on Sepabeads EC-HA and its efficient application in continuous High Fructose Syrup production using packed bed reactor. **2019**, 125710.
47. Ang, L.F.; Por, L.Y.; Yam, M.F.J.P.O. Study on Different Molecular Weights of Chitosan as an Immobilization Matrix for a Glucose Biosensor. **2013**, *8*.

© 2025 by the author(s). Distributed under a Creative Commons CC BY license.

Preprints.org (www.preprints.org) | NOT PEER-REVIEWED | Posted: 3 June 2025 doi:10.20944/preprints202506.0243.v1

48. Yuan, Y.; Shen, J.; Salmon, S.J.M. Developing Enzyme Immobilization with Fibrous Membranes: Longevity and Characterization Considerations. **2023**, *13*.
49. Zhang, Y.; Chen, M.; Lu, J.; Li, W.; Wolynes, P.G.; Wang, W.J.T.J.o.P.C.B. Frustration and the Kinetic Repartitioning Mechanism of Substrate Inhibition in Enzyme Catalysis. **2022**, *126*, 6792 - 6801.
50. Aranaz, I.; Alcántara, A.R.; Civera, M.C.; Arias, C.; Elorza, B.; Heras Caballero, A.; Acosta, N.J.P. Chitosan: An Overview of Its Properties and Applications. **2021**, *13*.
51. Courtecuisse, E.; Bourasseau, S.; Christensen, B.E.; Schatz, C.J.C.p. Synthesis of linear chitosan-block-dextran copolysaccharides with dihydrazide and dioxyamine linkers. **2024**, *345*, 122576.
52. da S Pereira, A.; Souza, C.P.L.; Moraes, L.B.D.d.; Fontes-Sant'Ana, G.C.; Amaral, P.F.F.J.P. Polymers as Encapsulating Agents and Delivery Vehicles of Enzymes. **2021**, *13*.
53. Ayers, M.R.; Hunt, A.J.J.J.o.N.-c.S. Synthesis and properties of chitosan–silica hybrid aerogels. **2001**, *285*, 123-127.
54. Yang, J.; Fan, D.; Zhao, F.; Lin, Y.; Zheng, S.; Han, S.J.F.i.B.; Biotechnology. Characterization of D-Allulose-3-Epimerase From Ruminiclostridium papyrosolvens and Immobilization Within Metal-Organic Frameworks. **2022**, *10*.
55. Sadaqat, B.; Sha, C.; Dar, M.A.; Dhanavade, M.J.; Sonawane, K.D.; Mohamed, H.; Shao, W.; Song, Y.J.B. Modifying Thermostability and Reusability of Hyperthermophilic Mannanase by Immobilization on Glutaraldehyde Cross-Linked Chitosan Beads. **2022**, *12*.
56. Ray, A.K.; B, V.; Anwar Bég, O.; Gorla, R.S.R.; Murthy, P.V.S.N.J.I.J.o.N.M.f.H.; Flow, F. Magneto-bioconvection flow of a casson thin film with nanoparticles over an unsteady stretching sheet. **2019**.

Disclaimer/Publisher's Note: The statements, opinions and data contained in all publications are solely those of the individual author(s) and contributor(s) and not of MDPI and/or the editor(s). MDPI and/or the editor(s) disclaim responsibility for any injury to people or property resulting from any ideas, methods, instructions or products referred to in the content.

© 2025 by the author(s). Distributed under a Creative Commons CC BY license.